

Wood residue reuse for a synthesis of lignocellulosic biosorbent: characterization and application for simultaneous removal of copper (II), Reactive Blue 19 and cyprodinil from water

Nena Velinov, Jelena Mitrović, Miloš Kostić, Miljana Radović, Milica Petrović, Danijela Bojić & Aleksandar Bojić

Wood Science and Technology
Journal of the International Academy of
Wood Science

ISSN 0043-7719
Volume 53
Number 3

Wood Sci Technol (2019) 53:619-647
DOI 10.1007/s00226-019-01093-0



Your article is protected by copyright and all rights are held exclusively by Springer-Verlag GmbH Germany, part of Springer Nature. This e-offprint is for personal use only and shall not be self-archived in electronic repositories. If you wish to self-archive your article, please use the accepted manuscript version for posting on your own website. You may further deposit the accepted manuscript version in any repository, provided it is only made publicly available 12 months after official publication or later and provided acknowledgement is given to the original source of publication and a link is inserted to the published article on Springer's website. The link must be accompanied by the following text: "The final publication is available at link.springer.com".



Wood residue reuse for a synthesis of lignocellulosic biosorbent: characterization and application for simultaneous removal of copper (II), Reactive Blue 19 and cyprodinil from water

Nena Velinov¹ · Jelena Mitrović¹ · Miloš Kostić¹ · Miljana Radović¹ · Milica Petrović¹ · Danijela Bojić¹ · Aleksandar Bojić¹

Received: 19 June 2018 / Published online: 9 April 2019
© Springer-Verlag GmbH Germany, part of Springer Nature 2019

Abstract

A new lignocellulosic- Al_2O_3 hybrid biosorbent (LC- Al_2O_3) was synthesized using wood residue material from the oak tree (*Quercus robur*). Biosorbent was tested for the simultaneous removal of three different types of pollutants: cationic (copper (II) ions), anionic (textile dye Reactive Blue 19) and nonpolar (fungicide cyprodinil) in the multi-component model solution and natural water. Biosorbent characterization was performed by Fourier transform infrared spectroscopy, scanning electron microscopy with energy-dispersive X-ray spectroscopy (SEM–EDX) and X-ray diffraction analysis. In order to define optimal process parameters for simultaneous removal of all three pollutants, effects of pH, temperature, sorbent dose, pollutants concentration and hydrodynamic conditions on the sorption process were investigated. Sorption of pollutants onto LC- Al_2O_3 was highly pH-dependent and the optimal pH is 5, with removal efficiency near 98% for all three pollutants. Sorption kinetics followed pseudo-second-order, intraparticle diffusion and Chrastil's models, which suggest that both surface reaction and diffusion were rate-limiting steps. Equilibrium experimental results are the best fitted by the Langmuir sorption isotherm model. The maximal sorption capacities of the biosorbent for simultaneous removal of pollutants in multi-component system are 15.69 mg g⁻¹ for copper (II), 29.99 mg g⁻¹ for Reactive Blue 19 and 20.97 mg g⁻¹ for cyprodinil. The present study shows that using wood residue material to produce a low-cost sorbent can reduce wood waste and increase reuse/recycling options, and also effectively decrease the water pollution simultaneously removing heavy metal ion, textile dye and pesticide from aqueous model solution and contaminated river water.

Electronic supplementary material The online version of this article (<https://doi.org/10.1007/s00226-019-01093-0>) contains supplementary material, which is available to authorized users.

✉ Nena Velinov
nena.velinov@yahoo.com

¹ Department of Chemistry, Faculty of Sciences and Mathematics, University of Niš, 33 Višegradska St, Niš 18000, Serbia

Introduction

Water pollution is one of the greatest crises facing the world. The largest source of it is the sewage water without treatment, as well as water coming from pesticide-ridden fields, and chemical waste produced by small and big industries (Albadarin et al. 2017). Two of the most basic environmental pollutants discharged to water or wastewaters are metals and dyes. Wastewaters contain various inorganic and organic contaminants, which could pose risks to the environment and public health. They not only contain high toxicity and color the water body but also seriously retard photosynthesis and inhibit a normal growth of aquatic organisms (Lazar 2005). Many industries (employed with dyestuffs, textile, paper and plastics) use dyes in order to colorize their products and generate a considerable amount of colored wastewaters. Furthermore, waste streams from metal cleaning and plating facilities and electronic device manufactures may contain a considerable amount of toxic heavy metals. To avoid these adverse effects, wastewater must be treated prior to its final discharge into the receiving environment. Unfortunately, incomplete removal has often been reported for these contaminants in wastewater by conventional wastewater treatment technologies.

Among the numerous techniques regarding the removal of environmental pollutants, sorption has been found to be a superior technique as compared to other methods of wastewater treatment in terms of cost, the simplicity of design and operation, availability, effectiveness and insensitivity to toxic substances (Amirnia et al. 2016; Bektaş et al. 2011; Daneshvar et al. 2017; Todorcius et al. 2015). Sorption, as one of the most promising techniques, can be used to remove different types of pollutants as dyes, pesticides, heavy metals and many other (Alqadami et al. 2017, 2018; Bektaş et al. 2011; Daneshvar et al. 2017; Javadian et al. 2014; Naushad et al. 2015, 2017; Todorcius et al. 2015).

Numerous works present results on the sorption of different types of either inorganic or organic pollutants on the various sorbents but in the single-component aqueous solutions (Alqadami et al. 2017, 2018; Bektaş et al. 2011; Daneshvar et al. 2017; Javadian et al. 2014; Naushad et al. 2015, 2017; Todorcius et al. 2015). Going to more specific/complicated studies, limited works have been published dealing with the sorption of same-type pollutants in multi-component aqueous systems. In those works, the interactions/mechanisms (synergetic or competitive) among the same-type pollutants were attempted to be clarified (Albert et al. 2018; Akbari et al. 2015). A few other works reported on the simultaneous sorption of organic pollutant and heavy metals in the binary system (Huang et al. 2015; Jin et al. 2016; Kyzas et al. 2013; Li et al. 2016; Oyanedel-Craver et al. 2007). However, there is no general rule for the simultaneous sorption of a heavy metal ion and an organic molecule. On the contrary, the mutual effects depend on the particular structure of the dyestuff, metal and sorbent. In some synergetic cases of sorption, there is no effect of metal on organic molecule sorption (Deng et al. 2013; Huang et al. 2015; Jin et al. 2016; Oyanedel-Craver et al. 2007). On the other hand, there is a competition (antagonism) between metal and organic pollutant for the sorption sites (Deng et al. 2013; Kyzas et al.

2013; Li et al. 2016). In one specific case of multi-component system of three pollutants, the sorbent could remove only two pollutants in the single-component system, but simultaneously remove all three pollutants in the three-component system, because of the interaction and complexation between pollutants (Ma et al. 2016a, b).

In the current work, the coexistence of different-type pollutants, two organic [textile dye Reactive Blue 19 (RB19) and pesticide cyprodinil] and one inorganic [copper (II) ions], in a triplet aqueous system is under consideration. The idea for the coexistence of heavy metal, reactive dye and pesticide has a real environmental meaning, because apart from dyes and heavy metals from industry, other potentially problematic contaminants are pesticides and their leaching to groundwater (Pionke and Glotfelty 1990). Thus, it is ideal and practical to simultaneously remove three completely different types of pollutants: cationic copper (II) ion, anionic reactive dye molecule and nonpolar cyprodinil molecule from natural water and wastewaters without interaction between them.

As biosorbent hybrid material, chemically modified lignocellulosic biomass with a small amount of Al_2O_3 (LC- Al_2O_3) was used. As a starting biomass, woodchips from an oak tree (*Quercus robur*) with lignocellulosic structure, mainly consisting of 46% cellulose and 24% of lignin, were used (Pettersen 1984). Woodchips were generated from wood industries, particularly from furniture manufacturing, so in that manner we can reduce waste and increase reuse/recycle options of woodchips.

Therefore, the novelty of this study was dedicated to using a wood residue industrial material to produce a low-cost sorbent material, which can effectively be used in the field of wastewater treatment and waste recycling management, to simultaneously remove three completely different types of pollutants from natural and wastewaters. Firstly, LC- Al_2O_3 hybrid was used to remove Cu(II) ions, RB19 and cyprodinil from single-component aqueous solutions in order to investigate principal operational process parameters (pH of the solution, temperature, sorbent dose, pollutants concentration and hydrodynamic conditions) and optimize the sorption process. Then, under the optimal parameter conditions, a simultaneous removal of three pollutants in a multi-component system was done. Appropriate common kinetics, isotherm and thermodynamic models that use various parameters, were applied to determine the sorption mechanism, equilibrium and sorbent capacity.

Materials and methods

Materials

$Cu(NO_3)_2 \cdot 3H_2O$, RB19 and cyprodinil were purchased from Sigma-Aldrich. $Al(NO_3)_3 \cdot 9H_2O$, HNO_3 and NaOH were of reagent grade (Merck, Germany). All chemicals were used without further purification. All solutions were prepared with deionized water (18 M Ω).

Preparation and characterization of biosorbent

The experiments were performed using a woodchips residue generated from an oak tree (*Quercus robur*), which was fractionated by size and washed with deionized water. 10 g of lignocellulosic biomass was acid-treated (0.3 M HNO₃) to remove bio-accumulated metals and then alkali-treated (1 M NaOH) for 60 min. After that, the material was mixed with a solution of 1 g of Al(NO₃)₃ × 9H₂O dissolved in 100 cm⁻³ of deionized water. The suspension was stirred for 0.5 h at 25.0 ± 0.5 °C, and then, the solution was evaporated. The obtained material was washed with deionized water and treated by trimethylamine, and then washed with deionized water until neutral pH and dried at 55 ± 1 °C for 5 h. This material was abbreviated as LC-Al₂O₃.

The content of Al in the biosorbent was determined using ICP-OES model iCAP 6500 Duo (Thermo Scientific, UK) equipped with a CID86 chip detector. SEM was performed using the JEOL JSM-5300 equipped with EDS LINK QX 2000 ANALYTICAL. For SEM–EDX analysis, samples were attached to aluminum stubs using Agar carbon tabs. A JEOL5310LV was used for imaging the samples in low vacuum mode with an Oxford Instruments X-Max 50 detector for semi-quantitative EDX analysis. Samples were imaged uncoated. Nominal magnifications of ×5.0 k, 10.0 k and 25.0 k were used when imaging the samples. Three random particles were averaged for EDX analysis. FTIR spectra were recorded by means of BOMEM MB-100 FTIR spectrometer (Hartmann & Braun, Canada) using KBr pellets containing 1.0 mg of the sample in 150 mg KBr. The instrument was equipped with a standard DTGS/KBr detector in the range of 4000–400 cm⁻¹ with a resolution of 2 cm⁻¹. The crystal structure was analyzed by XRD using filtered Cu Kα radiation (Ultima IV Rigaku). The experiments were performed in the scan range 2θ = 5–90° under 40 kV, 40 mA, with scan speed 5 degree/min and steps with 0.02°. Prior to the measurement, the angular correction was done by a high-quality Si standard. Lattice parameters were refined from the data using the least square procedure. The standard deviation was about 1%. The specific surface area was measured by a nitrogen adsorption using the Micromeritics Gemini 5 Surface Area Analyzer, USA. The sample was degassed under flowing nitrogen at 90° C overnight.

Batch sorption experiments

Working model solutions of Cu(II) ions and RB19 were prepared by the appropriate dilution of the stock solutions (0.1000 g dm⁻³). Working model solutions of cyprodinil were prepared by the appropriate dilution of the stock solutions (0.1000 g dm⁻³) in 10% ethanol. The pH of the solutions was adjusted with 0.1/0.01 mol dm⁻³ NaOH/HNO₃ solutions pH-metrically (Orion Star A214, Thermo Fisher Scientific, USA). In order to maintain a certain temperature, all experiments were carried out in the water bath by recirculating water from a thermostatic bath Julabo F12-ED (Refrigerated/

Heating Circulator, Germany). In order to examine the hydrodynamic conditions and ultrasound power effect, experiments were conducted in an ultrasonic bath (Sonic, Serbia; total nominal power: 50 W) that operates at 40 kHz frequency. The aliquots of the solution were taken before the sorption started and after particular periods of time.

The concentrations of Cu(II) ions in the solution were determined by an atomic adsorption spectrometer Analyst AA 300 (PerkinElmer, USA). Dye concentration was measured using UV–Vis spectrophotometer UV-1800 (Shimadzu, Japan) at 592 nm. Cyprodinil concentration was determined using the Dionex Ultimate 3000 HPLC system (Thermo Scientific, USA). The limit of detection (LOD) for cyprodinil is approximately 0.03 ppm (Vaquero-Fernandez et al. 2008).

The amount of sorbed pollutants q_t (mg g^{-1}) and the removal efficiency of pollutants (RE) were determined by using the equations:

$$q_t = \frac{(c_0 - c_t) \cdot V}{m_s}$$

$$\text{RE (\%)} = \frac{c_0 - c_t}{c_0} \cdot 100$$

where c_0 and c_t are the initial and final pollutant concentrations (mg dm^{-3}), V is the solution volume (dm^3), and m is the mass of the sorbent (g).

Relative deviation (RD) and mean relative deviation (MRD) were calculated using the equations:

$$\text{RD} = \frac{|q_{\text{exp}} - q_{\text{cal}}|}{q_{\text{exp}}} \cdot 100\%$$

$$\text{MRD} = \frac{\sum |q_{\text{exp}} - q_{\text{cal}}|}{i}$$

where q_{exp} and q_{cal} are experimental and calculated values of the amount of sorbed pollutant and i is the number of points. Kinetic, isotherm and thermodynamic studies were performed by preparing solutions with the initial concentration of Cu(II) ions, RB19 and cyprodinil in the range from 5.0 to 100.0 mg dm^{-3} , and mixing the solutions with 2.0 g dm^{-3} of the sorbent followed by agitating the mixture (pH 5.0, 150 rpm, at 25.0 °C) till equilibrium. All experiments were performed in triplicate. Average values \pm SD (error bars) are presented in all graphs. All parameters were evaluated with the nonlinear regression method by means of OriginPro 2016 software (OriginLab Corporation, USA).

Results and discussion

Material characterization

The SEM images of LC and LC-Al₂O₃ (Fig. 1) show a porous morphology of the biomaterial. The surface structure of the lignocellulosic biomass (Fig. 1a) and LC-Al₂O₃ biosorbent before (Fig. 1b) and after sorption of pollutants (Fig. 1c) is very similar, indicating that the modification process did not bring any significant change of the morphological structure of the material surface. The surface of the LC-Al₂O₃ biosorbent before and after sorption of Cu(II) ions, RB19 and ciprodinil is smooth, with characteristic channels and macropores, like those of basic lignocellulosic material. The sample had particle sizes above 1 mm and consisted of cell-like structures of around 100 μm in size. These structures have holes of around 1 μm in a random position over the cell-like units. Visible Al₂O₃ layers or particles as a separate phase on the biomaterial surface were not detected, which indicates that Al₂O₃ was highly and homogeneously dispersed, without a change in the biomaterial structure.

EDX analysis (Fig. 1) shows the presence of carbon and oxygen in unmodified biomass (Fig. 1a) and carbon and oxygen with aluminum in LC-Al₂O₃ biosorbent (Fig. 1b). Based on weight percentage quantification of samples, there are 53.1% of carbon and 46.9% of oxygen in the biomaterial before modification and 32.8% of carbon, 52.5% of oxygen, and 14.7% of aluminum in LC-Al₂O₃ biosorbent. The content of aluminum in the LC-Al₂O₃ biosorbent is in agreement with the results obtained by the ICP-OES method (14.68%).

The FTIR spectrum of the chemically modified lignocellulosic biomass is shown in Fig. 2. Modification of the lignocellulosic biomass by Al₂O₃ generates several changes in the IR region of 4000–400 cm⁻¹, which can predict the interaction of Al with cellulose O–H groups. Firstly, there is a slight displacement of the band from 3432 to 3424 cm⁻¹ associated with the O–H stretching vibration, indicating a reduced presence of hydrogen bonds and the loss of some O–H groups, probably due to the interaction of Al with O–, which was also confirmed by a decrease in the intensity of the band at around 3266 cm⁻¹ (Ayoob et al. 2007).

The band of unmodified biomass spectrum at around 2897 cm⁻¹ originating from symmetric C–H in R₃–C–H disappears in spectra of modified LC, so the methylene –CH₂ groups from asymmetric and symmetric C–H vibrations at about 2924 and 2855 cm⁻¹ are noticed more clearly. This phenomenon is characteristic for changes in cellulose starting crystallinity in the structure of lignocellulosic material, probably due to chemical treatment and reaction with Al.

Moreover, there is a slight displacement of the band associated with the O–H deformation mode, from 1632 to 1623 cm⁻¹. The decrease in intensity of the bands at around 1425 and 1330 cm⁻¹ associated with deformation vibration of the O–H group from CH₂–OH groups is also probably due to the interaction of Al with these centers of lignocellulosic biomass (Vazquez-Guerrero et al. 2016).

In addition, the band in unmodified biomass spectrum at around 781 cm⁻¹ originating from asymmetric C=O deformation disappears in spectra of modified

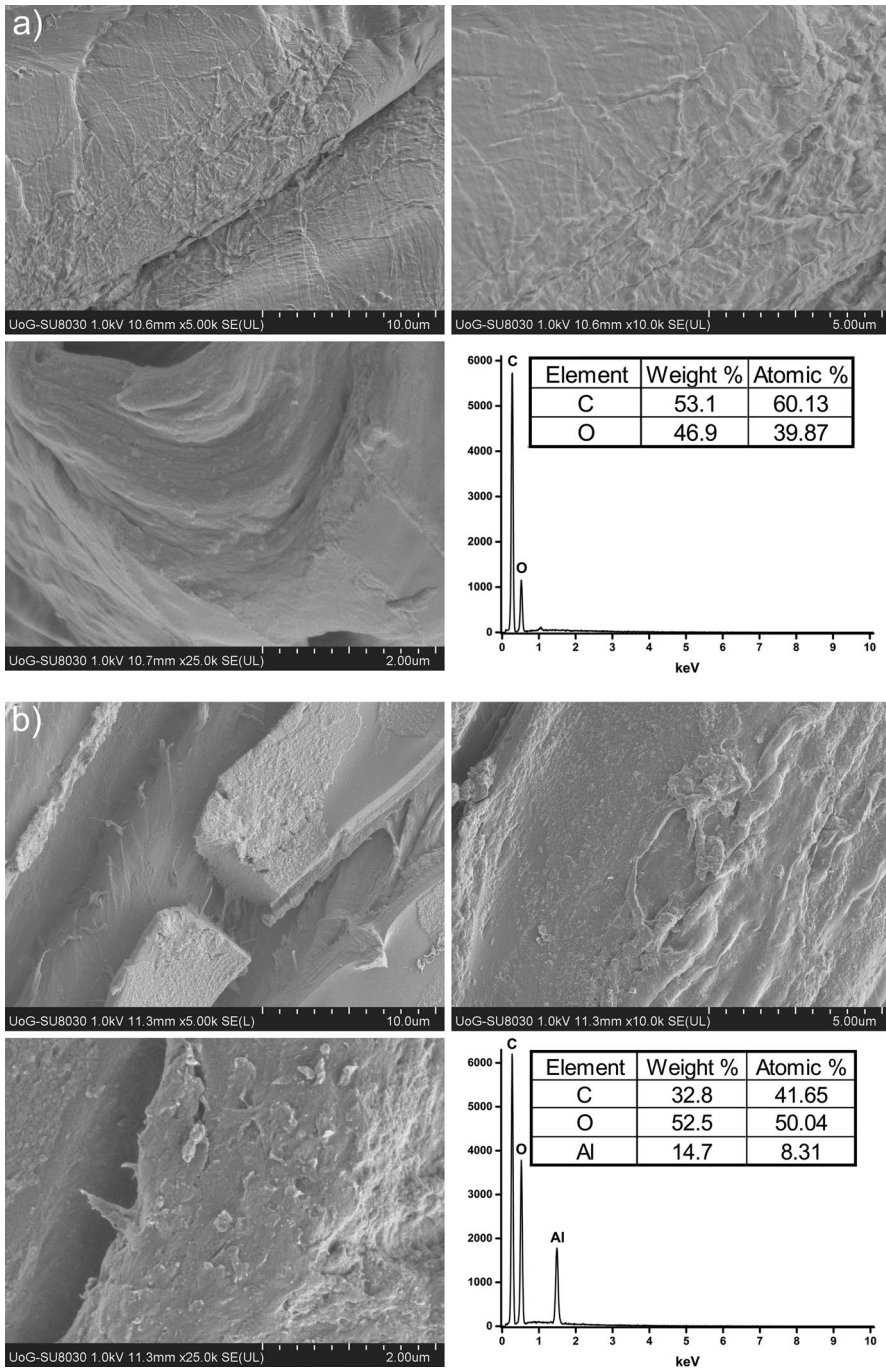


Fig. 1 SEM images with EDX spectrum of **a** unmodified biomass and **b** LC-Al₂O₃ biosorbent and **c** SEM image of LC-Al₂O₃ biosorbent after sorption

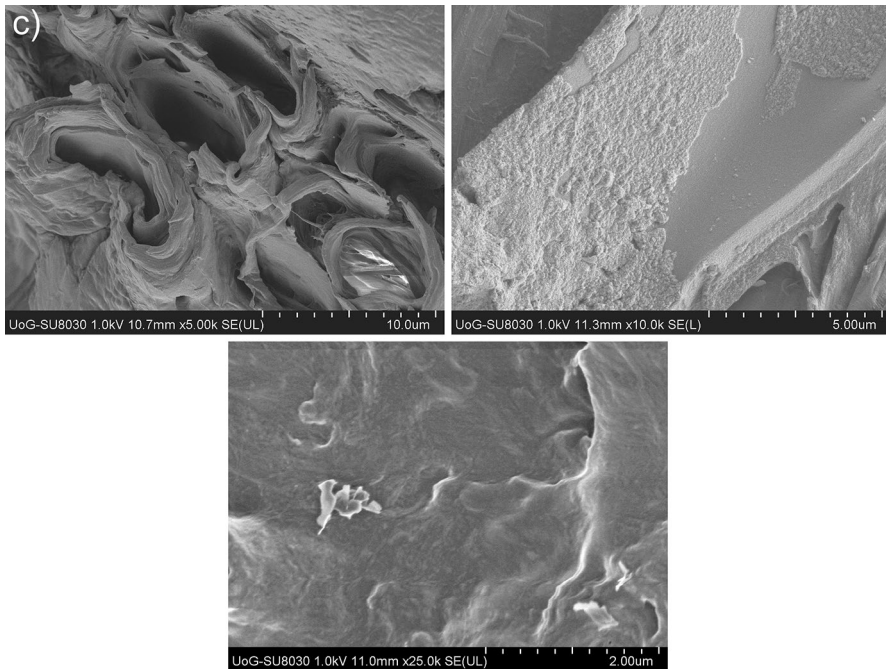


Fig. 1 (continued)

LC, so it is quite possible that Al (C–O–Al) bonding occurs at these centers. Distinct changes in the FTIR spectrum of the modified biosorbent are noted in the region $700\text{--}400\text{ cm}^{-1}$. The O–H out-of-plane bending vibrations in this area have a higher absorbance intensity ratio for higher substituted samples (El-Sakhawy 2001). This area indicates a higher occupation of the alumina octahedral sites, corresponding to Al–O vibration. These sites have a higher coordination, and their occupation will be favored by specified synthesis.

The spectra of the LC- Al_2O_3 biosorbent after sorption of the pollutants (Fig. 2) showed similar characteristics to the biosorbent before sorption except for slight changes. The FTIR spectrum of the LC- Al_2O_3 biosorbent after sorption indicates that the peaks are slightly shifted from their position and the intensity is altered. These results indicated the involvement of some functional groups in the sorption process, through weak electrostatic interaction, so there is probably no possibility of chemical bonding in this process.

The XRD pattern of LC- Al_2O_3 shows the peaks that are typical for lignocellulosic materials with an amorphous structure (Fig. A1 in Online Resource). The XRD pattern of the biosorbent does not contain any characteristic peak of Al_2O_3 , which appears in the XRD spectra of different crystalline alumina (Kumar et al. 1999). Obtained XRD results mean that Al_2O_3 does not appear as an individual phase.

The results of the XRD analysis of LC- Al_2O_3 is in accordance with the result obtained by SEM–EDX analysis, which did not detect Al_2O_3 as a separate phase on the biosorbent surface. It can be assumed that LC- Al_2O_3 is a unique, highly

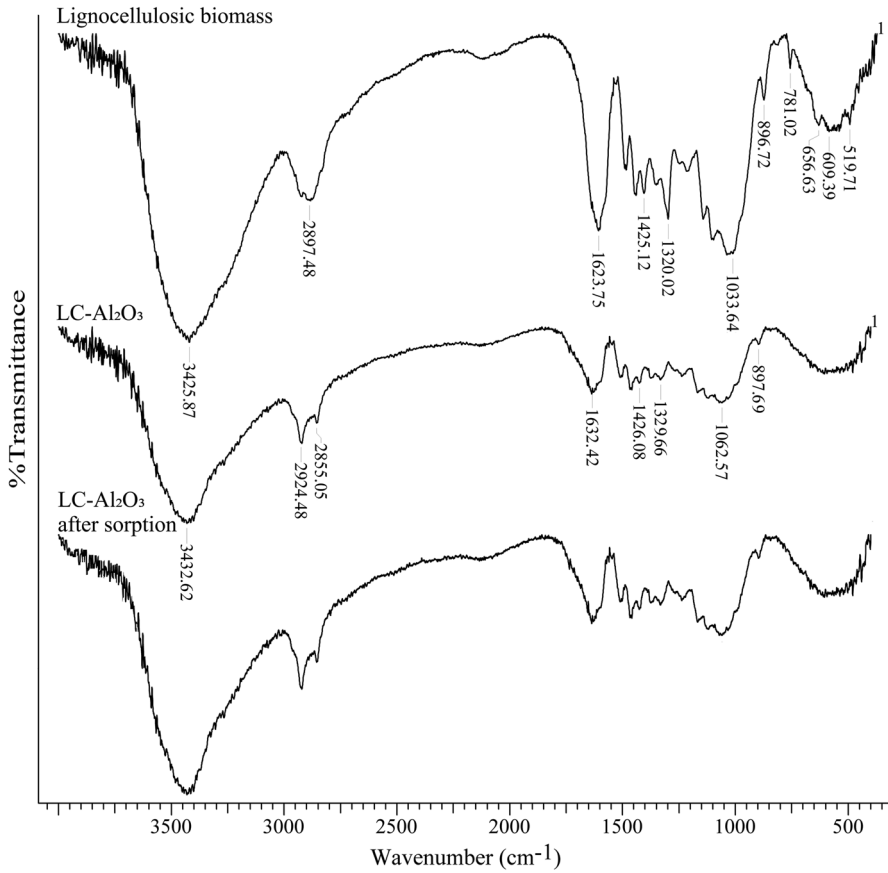


Fig. 2 FTIR spectra of unmodified biomass and LC- Al_2O_3 biosorbent before and after sorption

amorphous lignocellulosic material, where Al_2O_3 is bound to the biomass. This fact, as well as its absorption bands presented in the FTIR spectrum of LC- Al_2O_3 , indicates that it is chemically bonded to the biomaterial functional groups creating new specific active centers.

The specific surface area was estimated using the BET method. Surface area measurements of lignocellulosic biomass and LC- Al_2O_3 biosorbent before and after sorption of Cu(II) ions, RB19 and cyprodinil are presented in *Table A1 and Fig. A2 in Online Resource*. The BET results showed that lignocellulosic biomass has a higher pore volume and higher pore size compared with LC- Al_2O_3 biosorbent. Lignocellulosic biomass has a BET surface area of $5.71 \text{ m}^2 \text{ g}^{-1}$ with a broad BJH (Barrett–Joyner–Halenda) pore size distribution 5.13 nm, while LC- Al_2O_3 biosorbent has a BET surface area of $7.16 \text{ m}^2 \text{ g}^{-1}$ with a broad BJH pore size distribution 3.50 nm. After sorption of pollutants, the LC- Al_2O_3 biosorbent has a slightly lower BET surface area ($7.01 \text{ m}^2 \text{ g}^{-1}$) probably because of binding of pollutants on the functional groups of the biosorbent.

Optimization

Effect of pH

The removal of pollutants by LC- Al_2O_3 is significantly affected by the pH value of the solution, thereby changing the surface charge of the sorbent and the chemistry of the pollutants. Depending on surface charge of biosorbent and molecular charge of pollutants, sorption of the molecules on the surface may take place. The pH of the point of zero charge (pH_{pzc}) of LC- Al_2O_3 has been found to be 5.85. At pH below the pH_{pzc} , the sorbent surface is positively charged, and generally, anion sorption occurs. Otherwise, it would show a negative charge, so that the extent of sorption of cations increased.

In order to define the optimal pH value, where all three types of pollutants can be simultaneously removed with success from aqueous solution, the effect of the initial pH was examined in single-component aqueous solution by varying initial pH value from 2.0 up to 10.0, while other parameters were kept constant (initial pollutant concentration 20.0 mg dm^{-3} , sorbent dose 2.0 g dm^{-3} and temperature $25.0 \pm 0.2 \text{ }^\circ\text{C}$). The results are presented in Fig. 3.

Results show that an increase in the solution pH from 2 to 6 led to an increase in the removal efficiency of cationic pollutant Cu(II) ions from 35.05 to 99.08%. An increase in the solution pH from 2 to 5 led to a slight decrease in the removal efficiency of anionic pollutant RB19 from 99.91 to 97.90%, and with further increase up to 10 to a considerable decrease to 2.11%. With the increase in the solution pH from 2 to 5, removal efficiency of the nonpolar pollutant cyprodinil slightly increased from 91.08 to 98.18% and with a further increase in pH to 6,

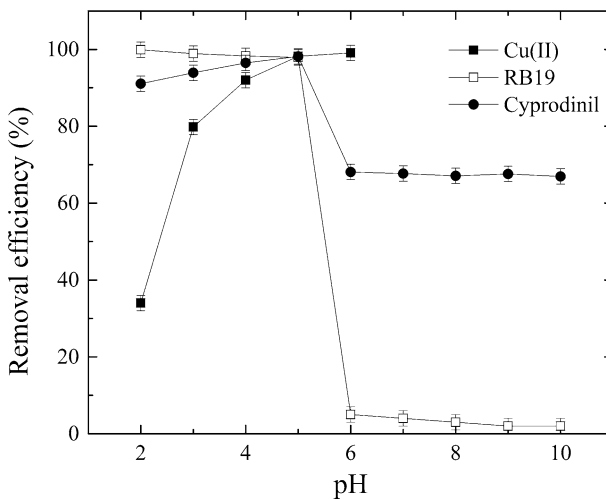


Fig. 3 Effect of pH on the removal of Cu(II) ions, RB19 and cyprodinil with LC- Al_2O_3 . Initial pollutant concentration 20.0 mg dm^{-3} , sorbent dose 2.0 g dm^{-3} , temperature $25.0 \pm 0.2 \text{ }^\circ\text{C}$

removal efficiency decreased to 68.08%, and after that a slight decrease reaching a minimum at pH 10 with a value of 66.91%.

Therefore, in the case of cationic pollutants, like Cu(II) ions, when the pH decreased, concentrations of protons increased and competition in binding the active sites on the surface of biosorbent, between the H^+ and metal ions started. Protonated active sites were incapable of binding metal ions, leading to free ions remaining in the solution. With the increase in pH, the overall surface on $LC-Al_2O_3$ became negative and sorption was increased and the competing effect of hydronium ions decreased. Dominant species of copper in the pH range 3–5 are Cu^{2+} and $CuOH^+$, while the copper at above 6.3 occurs as insoluble $Cu(OH)_2(s)$, so above pH 6, insoluble copper hydroxide starts precipitating from the solution and experiments could not be done (Akbari et al. 2015; Todorciuc et al. 2015).

In the case of the anionic pollutant RB19 at pH values lower than pH_{pzc} , the attraction occurs between a sulfonic group of the dye molecule, which is negatively charged, even in highly acidic solutions, and the positively charged sorbent surface. With the increase in medium pH, the net positive charge of the sorbent surface decreases and the RB19 uptake decreases as well. At pH higher than pH_{pzc} , the sorbent surface becomes negatively charged, the RB19 binding rapidly decreases (Albardin et al. 2017; Kyzas et al. 2013).

In the case of the nonpolar pollutant cyprodinil, the influence of pH on the sorption process is significantly smaller, indicating the physical nature of the sorption mechanism. Slightly lower sorption of cyprodinil at lower pH is due to the presence of excess H^+ ions competing with cyprodinil molecules for the sorption sites. The pK_a of cyprodinil is 4.44 and cyprodinil molecule gets deprotonated at higher pH. Therefore, in the pH range 4.44–5.85 ($pK_a - pH_{pzc}$), the sorbent surface is positively charged and cyprodinil is in the form of an anion, achieving best removal of cyprodinil, indicating the presence of chemical interactions between the sorbate and the material. At pHs above pH_{pzc} , a repulsive force occurs between the negatively charged cyprodinil molecules and negatively charged surface of biosorbent, and the removal efficiency of cyprodinil decreases. However, at higher pH values, the material has sorbed a significant amount of cyprodinil, indicating that ionic exchange is not a predominant sorption mechanism, though it is important. A similar trend for organic pollutants was reported by other authors (Chaudhuri et al. 2016; Roonasi and Nezhad 2016).

From the obtained results, it can be concluded that the optimal pH value, where all three types of pollutants can be simultaneously removed from water with highly significant removal efficiency, is 5, and the removal efficiency for Cu(II) ions, RB19 and cyprodinil at this pH is 98.21%, 97.9% and 98.18%, respectively. This pH value was also used for all further experiments.

Effect of temperature

The temperature of the solution plays an important role in the sorption process. Increasing the temperature is known to cause an increase in the rate of diffusion of the sorbate molecules across the external boundary layer and in the internal pores of

the sorbent, owing to the decrease in the viscosity of the solution. In that manner, changing the temperature will change the rate of the sorption (Javadian et al. 2014).

The experiments were done at different temperatures: 10.0, 20.0, 35.0 and 50.0 °C, while the other parameters were kept constant (initial pH 5.0, initial pollutant concentration 20.0 mg dm⁻³ and sorbent dose 2.0 g dm⁻³). Results show that an increase in the solution temperature from 10.0 to 50.0 °C led to an increase in the removal efficiency of ionic pollutants Cu(II) ions and RB19 by LC-Al₂O₃, indicating the process to be endothermic in nature. However, it led to a decrease in the removal efficiency of nonpolar pollutant cyprodinil (Fig. 4), indicating the process to be exothermic in nature. The removal efficiency increased from 84.12 to 99.9% for Cu(II) ions and from 90.67 to 99.9% for RB19, with an increasing temperature from 10.0 to 50.0 °C. Such influence of temperature may be a result of expected increase in the diffusion of Cu(II) ions and RB19 molecule in the water environment (Javadian et al. 2014; Naushad et al. 2015). With an increase in temperature from 10.0 to 50.0 °C, removal efficiency of cyprodinil decreases from 99.5 to 79.46%, which may be due to the physical nature of the sorption mechanism (Berrazoum et al. 2015). The optimal temperature for simultaneous removal of all three types of pollutants was 25.0 °C, where removal efficiency for Cu(II), RB19 and cyprodinil is 98.21%, 97.9% and 98.18%, respectively.

Effect of sorbent dose

The effect of sorbent dose on the removal efficiency of pollutants by LC-Al₂O₃ was investigated in the range from 0.5 to 8.0 g dm⁻³, while other parameters were kept constant (initial pH 5.0, initial pollutant concentration 20.0 mg dm⁻³ and temperature 25.0 ± 0.2 °C). The results are presented in Fig. 5. The effect of sorbent dose on

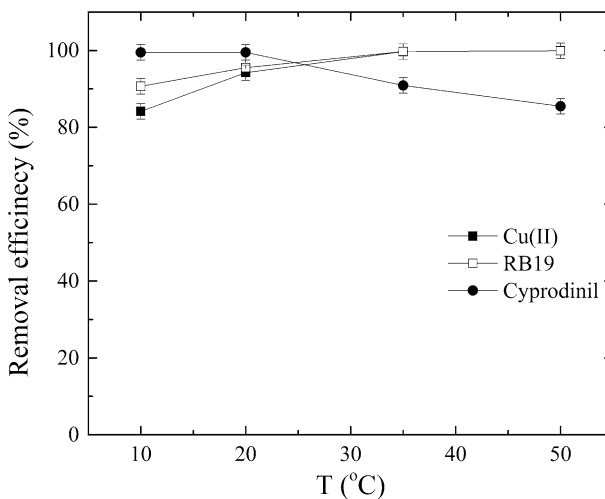


Fig. 4 Effect of temperature on the removal of Cu(II) ions, RB19 and cyprodinil with LC-Al₂O₃. Initial pH 5.00, initial pollutant concentration 20.0 mg dm⁻³, sorbent dose 2.0 g dm⁻³

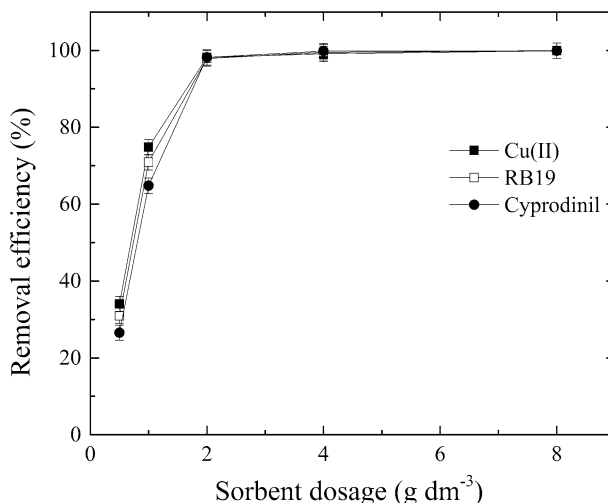


Fig. 5 Effect of sorbent dose on the removal of Cu(II) ions, RB19 and cyprodinil with LC-Al₂O₃. Initial pH 5.00, initial pollutant concentration 20.0 mg dm⁻³, temperature 25.0 ± 0.2 °C

the removal efficiency is almost same for all three types of pollutants. Removal efficiency of Cu(II) ions, RB19 and cyprodinil increased quickly from 34.05 to 98.21%, from 30.9 to 97.90%, and from 26.54 to 98.18%, respectively, with an increase in the sorbent dose from 0.5 to 2.0 g dm⁻³, because of the increased active surface area of the biosorbent and the number of available binding sites for pollutants. Further increase in the sorbent dose to 4.0 g dm⁻³ slightly enhanced removal efficiency to 99.1%, 99.5% and 99.8% for Cu(II) ions, RB19 and cyprodinil, respectively. The removal efficiency was without change at the sorbent doses of 6.0–8.0 g dm⁻³. A negligible change in the removal efficiency at a biosorbent dosage higher than 2.0 g dm⁻³ may be attributed to the presence of the excess of active centers for pollutants binding on the biosorbent surface, with regard to the amount of pollutants initial concentration. Therefore, a value of 2.0 g dm⁻³ was considered as the optimal biosorbent dose of LC-Al₂O₃ for removal of all three types of pollutants, and it is used in all other experiments. A similar effect was reported by other authors (Bozbas and Boz 2016; Tural et al. 2017).

Effect of initial pollutants concentration

The effect of initial pollutants concentration on their removal efficiency by LC-Al₂O₃ was investigated in the range from 5.0 to 100.0 mg dm⁻³ for all three types of pollutants, while other parameters were kept constant (initial pH 5.0, sorbent dose 2.0 g dm⁻³ and temperature 25.0 ± 0.2 °C) (Fig. A3 (a, b, c) in Online Resource). With an increase in initial pollutant concentration, removal efficiency decreased. For initial concentrations of Cu(II) ions, RB19 and cyprodinil from 5.0 to 20.0 mg dm⁻³, the removal efficiency was very high (99.11–98.21%, 98.00–97.90% and 99.2–98.18%, respectively). With further increase in concentrations to

50.0 mg dm⁻³, the removal efficiency slowly decreased. With the increase in the initial concentration of pollutants up to 100.0 mg dm⁻³, removal efficiency decreased, reaching a value of 31.38%, 59.98% and 41.93% for Cu(II), RB19 and cyprodinil, respectively.

In the case of a lower concentration range (5.0, 10.0 and 20.0 mg dm⁻³), the ratio of initial number of sorbate molecules to the available sorption sites is low, and the biosorption becomes independent of initial concentration, which enabled the 99% pollutant uptake. At higher investigated concentrations (up to 100.0 mg dm⁻³), a certain amount of molecules is left unsorbed in the solution due to a saturation of the limited available binding sites in the biomass. Therefore, the removal of pollutants depends on its initial concentration, as in the case of plenty of similar pollutants (Tural et al. 2017; Kallel et al. 2016).

However, the biosorption capacity of pollutants increases with increasing their initial concentrations (Fig. 6) and reaches 15.69, 29.99 and 20.97 mg g⁻¹, for Cu(II) ions, RB19 and cyprodinil, respectively, with 100.0 mg dm⁻³ initial concentration of pollutant and 2.0 g dm⁻³ dose of biosorbent. This can be attributed to the fact that the higher pollutant concentrations increase the overall mass transfer driving force and thus the pollutant uptakes onto the biosorbent (Todorciuc et al. 2015).

Effect of hydrodynamic conditions

The effect of hydrodynamic conditions was investigated at different ultrasound power between 0 and 50 W. Ultrasound through its mechanical waves has been used as a means of enhancing the sorption process. Ultrasonic waves strongly enhance mass transfer between two phases through reducing the thickness of a boundary layer at the solid phase, and thus, the diffusion is enhanced (Entezari and Soltani

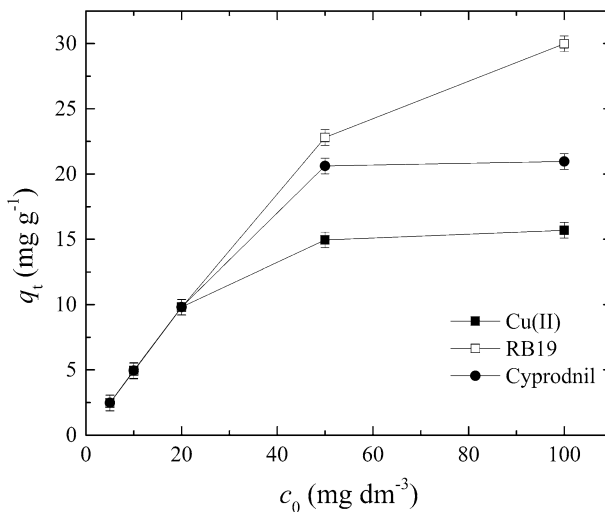


Fig. 6 Effect of initial pollutant concentration on the removal of Cu(II) ions, RB19 and cyprodinil with LC-Al₂O₃. Initial pH 5.0, sorbent dose 2.0 g dm⁻³, temperature 25.0 ± 0.2 °C

2008). The effect of hydrodynamic conditions on pollutants sorption was investigated at ultrasonic irradiation acoustic power of 0, 25 and 50 W, while other parameters were kept constant (initial pH 5.0, initial pollutant concentration 20.0 mg dm^{-3} , sorbent dose 2.0 g dm^{-3} and temperature $25.0 \pm 0.2 \text{ }^\circ\text{C}$) (Fig. A4(a, b, c) in Online Resource). It is clear from the results that the presence of ultrasound does not change the removal efficiency of any pollutant by LC- Al_2O_3 , but it speeds up the sorption process a lot. The removal efficiency in all three cases of different ultrasound power is 98.21%, 97.9% and 98.18% for Cu(II), RB19 and cyprodinil, respectively, but in the absence of ultrasound, the equilibrium is attained after 120 min. In the presence of ultrasound with powers of 25 and 50 W, the equilibrium is attained considerably faster (after 60 and 90 min for Cu(II) ion, after 20 and 60 min for RB19, and after 20 and 60 min for cyprodinil), through reducing the thickness of the boundary layer at the solid phase. The effect of the power of ultrasound has a greater impact on the sorption speed of RB19 and cyprodinil than Cu(II) ions, probably because of the size of the molecules. The stronger the acoustic power, the greater is the intensity of the ultrasonic field, which leads to the improvement of microstreaming, micro-turbulence, shock waves and microjets and to enhancement of mass transfer in the system and speeding up of the process of pollutants sorption, especially the sorption of larger molecules (Entezari and Soltani 2008).

Sorption kinetics

The kinetics of Cu(II) ions, RB19 and cyprodinil sorption on LC- Al_2O_3 hybrid can be described by the pseudo-first-order model, pseudo-second-order model, intraparticle diffusion model and Chrastil's diffusion model. The equations and parameters of all the above-mentioned kinetics models, along with their values and corresponding r^2 , are presented in Table 1.

Reaction kinetics

The pseudo-first-order kinetic model describes the rate of sorption, which is proportional to the number of unoccupied binding sites of the sorbent (Lagergren 1898). The pseudo-second-order kinetic model is based on equilibrium sorption, which depends on the amount of solute sorbed on the surface of sorbent and the amount sorbed at equilibrium (Ho and McKay 1998). In the nonlinear equations of the pseudo-first-order and pseudo-second-order kinetic models (Table 1), k_1 (min^{-1}) is the first-order rate constant, k_2 ($\text{g mg}^{-1} \text{ min}^{-1}$) is the second-order-rate constant, and q_t and q_e (mg g^{-1}) are the amounts of pollutant sorbed at time t and at equilibrium, respectively. The plot of q_t versus t for pseudo-first- and pseudo-second-order models for all three types of pollutant is shown in (Fig. A5(a, b) in Online Resource), respectively.

As can be seen from the data presented in Table 1, the determined values of q_e for both models showed similarity with the experimental values, but in the case of pseudo-second-order kinetic model, they are closer to the experimental q_e values. Obtained determination coefficients for pseudo-second-order model (0.989, 0.991

Table 1 Kinetic parameters for Cu(II), RB19 and cyprodinil sorption onto LC-Al₂O₃ biosorbent

Pollutant	Cu(II)	RB19	Cyprodinil
Pseudo-first-order model $q_t = q_c(1 - e^{-k_1 t})$			
q_e , exp (mg g ⁻¹)	9.82	9.79	9.82
q_e , cal (mg g ⁻¹)	9.08	9.23	9.39
k_1 (min ⁻¹)	0.08	0.10	0.05
r^2	0.964	0.965	0.981
RD (%)	7.54	5.72	4.38
MRD	1.95	1.93	1.97
Pseudo-second-order model $q_t = \frac{q_c^2 k_2 t}{1 + k_2 q_c t}$			
q_e , cal (mg g ⁻¹)	10.08	10.08	10.73
k_2 (g mg ⁻¹ min ⁻¹)	0.11	0.14	0.08
r^2	0.989	0.991	0.995
RD (%)	2.65	2.96	2.27
MRD	0.07	0.06	0.05
Intraparticle diffusion model $q_t = k_d t^{1/2} + C$			
k_{i1} (mg g ⁻¹ min ^{-1/2})	0.18	0.25	0.12
C_1 (mg g ⁻¹)	1.49	1.65	1.24
r^2	0.996	0.990	0.998
k_{i2} (mg g ⁻¹ min ^{-1/2})	0.25	0.17	0.14
C_2 (mg g ⁻¹)	6.55	7.56	7.96
r^2	0.988	0.997	0.980
Chrastil's diffusion model $q_t = q_c(1 - e^{-k_C A_0 t})^n$			
q_e , cal (mg g ⁻¹)	9.65	9.51	9.82
k_C	0.01	0.02	0.01
n	0.45	0.47	0.59
r^2	0.998	0.998	0.997

and 0.995) for Cu(II) ions, RB19 and cyprodinil, respectively, are relatively higher than the determination coefficients for pseudo-first-order model (0.964, 0.965 and 0.981). Obtained relative deviation for pseudo-second-order model (1.95, 1.93 and 1.97%) for Cu(II) ions, RB19 and cyprodinil, respectively, is lower than the relative deviation for pseudo-first-order model (7.54, 5.72 and 4.38%). In addition, the mean relative deviation for pseudo-second-order model (0.07, 0.06 and 0.05) for Cu(II) ions, RB19 and cyprodinil, respectively, is lower than the mean relative deviation for pseudo-first-order model (2.65, 2.96 and 2.27).

The experimental data showed that pseudo-second-order model better fitted experimental data than pseudo-first-order model for all three types of pollutants, due to a higher determination coefficient, better matching of experimental and calculated q_e values and lower values of relative deviation and mean relative deviation obtained in all cases. Obtained results indicate that the pseudo-second-order model can be successfully used for the study of Cu(II) ions, RB19 and cyprodinil sorption by LC-Al₂O₃ hybrid and suggest that the sorption process depends on the amount of solute

sorbed on the surface of sorbent and the amount sorbed at equilibrium (Alqadami et al. 2017; Naushad et al. 2017).

Diffusion kinetics

Intraparticle diffusion model: The sorbate transport from the solution phase to the surface of the sorbent particles occurs in several steps: bulk diffusion, external (film) diffusion, intraparticle diffusion and finally sorption of the sorbate onto the sorbent surface. The overall sorption process may be controlled by either one or more steps. The possibility of intraparticle diffusion was explored by using the intraparticle diffusion kinetics model (Weber and Morris 1964). In the equation of this model (Table 1), determined from a plot q_t versus $t^{1/2}$, the intercept is C , which gives an idea of the thickness of the boundary layer (the larger the intercept, the greater the boundary layer effect), and the slope is the intraparticle diffusion rate constant k_{id} ($\text{mg g}^{-1} \text{min}^{-1/2}$).

Regression of q_t versus $t^{1/2}$ for the sorption of Cu(II) ions, RB19 and cyprodinil onto LC- Al_2O_3 hybrid is not linear and showed multi-linearity and two stages in sorption, suggesting that the intraparticle diffusion is not the only rate-controlling step (Fig. A5c in Online Resource). The first, sharper portion of the plot can be attributed to the diffusion of molecules of the pollutants through the solution of the external sorbent surface, or the boundary layer diffusion of solute molecules. It is a rate-limiting process at the beginning of the sorption. The second portion described the gradual sorption stage, where intraparticle diffusion and finally sorption of the sorbate onto the sorbent surface were rate-limiting. Similar results were shown in the studies of other authors, who fitted kinetic data by two linear lines with a different slope (Liu et al. 2015; Shakib et al. 2017).

Based on values for intraparticle diffusion rate constants, k_{id1} and k_{id2} (Table 1) for all three pollutants, it can be concluded that film diffusion is more efficient than intraparticle diffusion, and the intraparticle diffusion is the rate-limiting step. In addition, the C_1 values for all three pollutants are lower than C_2 value (a measure of the thickness of the boundary layer) and a larger C value corresponds to a greater boundary layer diffusion effect, indicating decreases in the rate of the external mass transfer and hence increases in the rate of internal mass transfer.

Chrastil's diffusion model: Chrastil's diffusion model describes sorption kinetics in diffusion-controlled systems (Chrastil 1990). In the mathematical equation of this model (Table 1), k_C is a rate constant ($\text{dm}^3 \text{g}^{-1} \text{min}^{-1}$), which depends on diffusion coefficients and the sorption capacity of biosorbent, A_0 is the dose of biosorbent (g dm^{-3}) and n is a heterogeneous structural diffusion resistance constant, which can range from 0 to 1. Constant n is independent of the sorbate concentration, sorbent concentration A_0 , q_e and temperature. In systems with small diffusion resistance, parameter n approximates 1, while the more significant resistance parameter n assumes small values (<0.5). The plot of q_t versus t for all three types of pollutants is shown in Fig. A5d in Online Resource.

The high determination coefficients, obtained by a nonlinear regression analysis, are larger than 0.99 (Table 1) for all three types of pollutant, indicating a very good fit of experimental kinetic data with Chrastil's model. Applicability of this diffusion

model also confirms similar values of the calculated q_e with experimentally determined q_e (Table 1). The results obtained for the diffusion resistance coefficient show that n values are 0.45, 0.47 and 0.59 (Table 1) for Cu(II) ions, RB19 and cyprodinil, respectively. Low values of constants n mean that the sorption rate is strongly limited by the diffusion resistance.

Sorption isotherm

In this work, different biosorption equilibrium models (Langmuir, Freundlich and Sips) were evaluated to fit the experimental LC- Al_2O_3 biosorption of Cu(II) ions, RB19 and cyprodinil isotherms. The isotherm nonlinear equations and parameters, deduced from experimental data by a nonlinear regression of the plot q_e versus c_e (Fig. A6 (a, b, c) in Online Resource), for all the above-mentioned models, along with their values and corresponding r^2 are presented in Table 2, where q_e is the amount of sorbate sorbed at equilibrium ($mg\ g^{-1}$), c_e is the equilibrium concentration of the sorbate in solution ($mg\ dm^{-3}$), q_m is the maximum sorption capacity ($mg\ g^{-1}$), and K_L is a Langmuir constant related to the energy of sorption, which reflects quantitatively the affinity between the sorbate and the sorbent, K_f is Freundlich constant, related to the sorption capacity, and $1/n$ is Freundlich exponent, related to the intensity of sorption, which varies with the heterogeneity of the sorbent surface, K_S is the Sips equilibrium constant ($dm^3\ mg^{-1}$), and $1/n$ is the Sips model exponent.

The Langmuir model assumes that the uptake of adsorbate occurs on an energetically homogeneous surface by monolayer adsorption without any interaction between adsorbed species (Langmuir 1918; Ho and McKay 2000). The Freundlich empirical adsorption isotherm equation is based on adsorption on a heterogeneous surface. It is assumed that the stronger binding sites are occupied first and that the

Table 2 Isotherm parameters for Cu(II), RB19 and cyprodinil sorption onto LC- Al_2O_3 biosorbent

Adsorption isotherm	Parameter	Cu(II)	RB19	Cyprodinil
Langmuir $q_e = \frac{q_m K_L c_e}{1 + K_L c_e}$ $\theta = \frac{K_L c_0}{1 + K_L c_0}, R_L = \frac{1}{(1 + K_L c_0)}$	q_m ($mg\ g^{-1}$)	15.42	29.83	21.27
	K_L ($dm^3\ mg^{-1}$)	4.92	0.99	2.55
	r^2	0.997	0.991	0.997
	MRD	0.24	0.73	0.33
Freundlich $q_e = K_F c_e^{1/n}$	K_F , ($mg\ g^{-1}$) $^{1/n}$	8.40	11.57	10.42
	n	6.10	3.64	5.03
	r^2	0.834	0.87	0.819
	MRD	1.66	2.84	2.61
Sips $q_e = \frac{q_m K_S c_e^{1/n}}{1 + K_S c_e^{1/n}}$	q_m ($mg\ g^{-1}$)	15.41	31.40	21.54
	K_S ($dm^3\ mg^{-1}$)	4.95	0.78	2.35
	n	1.01	0.85	0.90
	r^2	0.995	0.993	0.998
	MRD	0.24	0.58	0.23

binding strength decreases with the increasing degree of site occupation (Freundlich 1906). The Sips isotherm is a combined form of Langmuir and Freundlich expressions used for predicting the heterogeneous adsorption systems and circumventing the limitation of the rising sorbate concentration associated with the Freundlich isotherm model (Sips 1948). At low sorbate concentrations, it reduces to the Freundlich isotherm, while at high concentrations, it predicts a monolayer sorption capacity characteristic of the Langmuir isotherm.

The highest determination coefficient ($r^2 > 0.99$) of the Langmuir model for all three pollutants indicates that the Langmuir model gives the best fit to the experimental data and thus, the nature of sorption of pollutants on the sorbents is more compatible with Langmuir assumptions about the monolayer sorption of the investigated pollutant on the sorbent, and after saturation of this layer, no further sorption took place.

The Langmuir isotherm shows that the amount of pollutant sorption increases as the concentration increases up to a saturation point. The maximum biosorbent capacity determined from the Langmuir isotherm model was 15.42, 29.83 and 21.27 mg g⁻¹ (Table 2) for Cu(II), RB19 and cyprodinil, respectively, which is consistent with the experimental value (15.69, 29.99 and 20.97 mg g⁻¹, respectively).

From Langmuir equilibrium constant (K_L), the Hall separation factor (R_L) and the surface coverage (θ) can be calculated (Table 2). The first is indicative of the biosorption isotherm shape that predicts whether a biosorption isotherm is: irreversible ($R_L = 0$), favorable ($0 < R_L < 1$), linear ($R_L = 1$) or unfavorable ($R_L > 1$), while the latter indicates the fraction of the biosorption sites occupied by pollutant at equilibrium.

The separation factor fell from 0.039 to 0.002, from 0.17 to 0.01 and from 0.078 to 0.003 as the initial pollutant concentration increased from 5.0 to 100.0 mg dm⁻³ for Cu(II), RB19 and cyprodinil, respectively, which indicates that the biosorption of these pollutants onto LC-Al₂O₃ increased as the initial concentration rose. Furthermore, the R_L values are between 0 and 1, indicating that the biosorption by LC-Al₂O₃ hybrid for all three pollutants is favorable at all assayed concentrations and confirming the suitability of the biosorbent for the sorbate (Naushad et al. 2015).

The surface coverage (θ) values approached unity (from 0.96 to 0.99, from 0.83 to 0.99 and from 0.93 to 0.99 for Cu(II), RB19 and cyprodinil, respectively) with increasing initial concentration of the pollutants, which indicates that the LC-Al₂O₃ surface was almost completely covered by a monomolecular layer of pollutant molecules at high concentrations of the pollutants. It is also apparent that the surface coverage ceased to vary significantly at higher concentrations of pollutants and that the reaction rate became almost independent from their concentrations. The θ values indicated effective biosorption of all three pollutants from aqueous solutions by LC-Al₂O₃ hybrid at all the assayed initial concentrations.

In the Freundlich isotherm model, if the value of the exponent $1/n = 1$, then the free energy for all sorbate concentrations is constant; if $1/n < 1$, that added sorbate is with weaker and weaker free energies; finally if $1/n > 1$, then more sorbate present in the sorbent enhances the free energies of further sorption. The parameter n is related to the sorption energy distribution: When $n = 1$, the partition between the two phases is independent of the concentration; when n lies between one and ten, this indicates

a favorable sorption process. From the data in Table 2, the values of n are 6.10, 3.64 and 5.03, for Cu(II), RB19 and cyprodinil, respectively, indicating that the sorption of all three pollutants onto LC- Al_2O_3 hybrid is favorable and the r^2 value is 0.834, 0.87 and 0.819, for Cu(II), RB19 and cyprodinil, respectively. These values also suggest the formation of an almost homogeneous surface.

The heterogeneity factor of n in Sips model close to or even 1 shows a biosorbent with comparatively homogenous binding sites, while n close to 0 displays heterogeneous biosorbents. In other words, if $n = 1$, then the Langmuir isotherm model will be the preferable one, while if $n = 0$, then the Freundlich isotherm will be preferred. Sips isotherm model has a very high r^2 value (0.995, 0.993 and 0.998) and almost the same q_m values (15.41, 31.40 and 21.54 mg g^{-1}) which is consistent with experimental values (15.69, 29.99 and 20.97 mg g^{-1}) for Cu(II), RB19 and cyprodinil, respectively. The values of the exponent of the Sips model n_s (1.01, 0.85 and 0.90 for Cu(II), RB19 and cyprodinil, respectively) were close to 1, meaning that the Sips model is effectively reduced to the Langmuir model (Todorciuc et al. 2015). In addition, the values of mean relative deviation are lower for the Langmuir and Sips model, and the highest for the Freundlich model, for all three pollutants. Thus, experimental equilibrium data for the biosorption of all three pollutants by LC- Al_2O_3 hybrid should preferably be fitted with the Langmuir model (Abdolali et al. 2015; Todorciuc et al. 2015).

Thermodynamics

Thermodynamic parameters, including the change in free energy (ΔG°), enthalpy (ΔH°) and entropy (ΔS°), were used to describe the thermodynamic behavior of the biosorption of Cu(II) ion, RB19 and cyprodinil on LC- Al_2O_3 hybrid. Thermodynamic parameters were calculated from the following equations:

$$\Delta G^\circ = \Delta H^\circ - T\Delta S^\circ$$

$$\ln K_D = \frac{\Delta S^\circ}{R} - \frac{\Delta H^\circ}{RT}$$

$$K_D = K_L \cdot M$$

where R is the universal gas constant (8.314 $\text{J mol}^{-1} \text{K}^{-1}$), T is temperature (K), K_D ($\text{dm}^3 \text{mmol}^{-1}$) is the distribution coefficient, K_L ($\text{dm}^3 \text{mg}^{-1}$) is the Langmuir equilibrium constant, and M (mg mol^{-1}) is the molar weight of pollutants (Bektaş et al. 2011; Liu 2006, 2009; Santos and Boaventura 2016). The experiments were carried out at 283, 293, 308 and 323 K. The enthalpy and the entropy change in biosorption were estimated from the slope and intercept of the linear regression of $\ln K_D$ versus $1/T$ plot (Fig. A7 in Online Resource). These thermodynamic parameters are given in Table 3. The negative values ΔG° in all three cases indicate the feasibility of the biosorption process and its spontaneous nature for all three pollutants. With the increase in temperature from 283 to 323 K, free energy decreases for the biosorption of Cu(II) ions and RB19, showing a slight increase in the feasibility of biosorption at higher temperatures. The decrease in ΔG° values with increase in

Table 3 Thermodynamic parameters for Cu(II), RB19 and cyprodinil sorption onto LC-Al₂O₃ biosorbent

Pollutant	ΔS° (J mol ⁻¹ K ⁻¹)	ΔH° (kJ mol ⁻¹)	ΔG° (kJ mol ⁻¹)			
			283 K	293 K	308 K	323 K
Cu(II)	266.11	59.52	-15.79	-18.45	-22.44	-26.43
RB19	247.00	56.23	-13.67	-16.14	-19.84	-23.54
Cyprodinil	9.60	-14.05	-11.33	-11.23	-11.09	-10.94

temperature shows a slight decrease in the feasibility of biosorption for cyprodinil at higher temperatures. The positive ΔH° (59.52 and 56.23 kJ mol⁻¹) value for Cu(II) and RB19, respectively, implies an endothermic character of the process of biosorption, and the negative ΔH° (-14.05 kJ mol⁻¹) value for cyprodinil implies an exothermic character of the process of biosorption within the analyzed range of temperatures (10.0–50.0 °C) (Bektaş et al. 2011; Wibowo et al. 2017). The enthalpy value within 2.1–20.9 kJ mol⁻¹ points to physical sorption, whereas the value from 80 to 200 kJ mol⁻¹ indicates chemisorption. Thus, the higher values of ΔH° for Cu(II) ion and RB19 indicate the physicochemical sorption process rather than a pure physical or chemical sorption process onto LC-Al₂O₃ hybrid of these pollutants. In the case of cyprodinil, based on the ΔH° , the sorption process should be attributed more to physical sorption. The positive ΔS° value for Cu(II) ion, RB19 and cyprodinil (Table 3) suggests an increase in the randomness at the solid/solution interface during the sorption by LC-Al₂O₃ hybrid and corroborates the previously proposed spontaneity of the biosorption process (Isah et al. 2015; Wibowo et al. 2017).

Applications of the LC-Al₂O₃ biosorbent

Simultaneous removal of Cu(II) ions, RB19 and cyprodinil from the aqueous model solution

Based on the results obtained by optimization of the biosorption process that has been made, the optimal dose of LC-Al₂O₃ hybrid needed for simultaneous removal of Cu(II), RB19 and cyprodinil was 2 g dm⁻³ in the model solution with initial pH 5 and temperature 25.0 °C. The concentration of Cu(II) ions, RB19 and cyprodinil in the sample was 20 mg dm⁻³ each. The results have shown that the simultaneous removal of all types of pollutants was very effective, and the removal efficiency for Cu(II) ions, RB19 and cyprodinil was the same as that achieved in single model solutions (98.21, 97.9 and 98.18%, respectively) indicating that there was no mutual influence of pollutants on each other. The high removal efficiency for all tested pollutants by LC-Al₂O₃ hybrid from water indicates the great application potential of this material for simultaneous removal of cationic, anionic and nonpolar pollutants.

Removal of Cu(II) ions, RB19 and cyprodinil from natural river water

To test the efficiency of LC-Al₂O₃ hybrid for removal of Cu(II) ions, RB19 and cyprodinil from water contaminated by those pollutants, the river water was used as the matrix for the sorption solution. River water contains various ions, which may affect the biosorbent process of the pollutants. After collecting, the river water was filtered through 0.45- μm filter in order to remove mechanical impurities and used as a matrix solution for the sorption process. Then, the river water matrix was contaminated with Cu(II) ions, RB19 and cyprodinil, while the concentration of every pollutant in the matrix was 20 mg dm⁻³. Based on the results obtained by optimization of the biosorption process, optimal parameters for the purification process were: initial pH 5 and temperature 25.0 °C, a dose of LC-Al₂O₃ hybrid 2 g for 1.0 dm⁻³ of the river water contaminated with all three types of pollutants. The results have shown that the removal efficiency for Cu(II) ions, RB19 and cyprodinil from contaminated river water was slightly lower than that achieved in model solutions (97.11, 95.72 and 96.47%, respectively), indicating that other components commonly present in the river water (Ca(II), Mg(II), organic matter, etc.) do not affect the sorption process to a large degree (approximately 2%), probably because of their small concentration in the river water and higher removal efficiency of the LC-Al₂O₃ sorbent for pollutants. The high removal efficiency of cyprodinil in river water by LC-Al₂O₃ biosorbent indicates the great application potential of the biosorbent in removing this kind of pollutants from water.

Removal of Cu(II) and RB19 from wastewater

The applicability of the LC-Al₂O₃ biosorbent was demonstrated by removing Cu(II) from copper plating industry wastewater. The metal content of copper plating industry effluent is shown in *Table A2 in Online Resource*. To prepare a working model solution, copper plating industry wastewater was diluted to 20.0 mg dm⁻³ of copper. The optimal parameters for biosorption process were: initial pH 5 and temperature 25.0 °C, dose of LC-Al₂O₃ hybrid 2 g for 1.0 dm⁻³ of the diluted copper wastewater solution. It was observed that the copper removal efficiency decreased by 15.86% compared to a single-metal solution of Cu(II) ions. Despite the presence of the competitive effect of other metal ions present in the wastewater, removal efficiency of Cu(II) ions was 82.35%, which is a significantly high value and indicates the great application potential of the biosorbent in removing metal cations from water.

In order to confirm the efficiency of the LC-Al₂O₃ biosorbent for the removal of RB19 in wastewater, a synthetic dye wastewater solution was made based on the real wastewater from dyeing process. The exact chemical composition of the synthetic dye bath used in the textile company is shown in *Table A3 in Online Resource*. The optimal parameters for the biosorption process were: initial pH 5 and temperature 25.0 °C, a dose of LC-Al₂O₃ hybrid 2 g for 1.0 dm⁻³ of the dye bath solution. The removal efficiency of RB19 decreased by 6.48% compared to a model solution of RB19 in deionized water, because of the presence of other components in the dyeing bath. In the synthetic dye wastewater, the removal efficiency was 91.42%, indicating that other components in day bath do not have a very significant competitive impact

on the biosorption process of dyes by LC- Al_2O_3 biosorbent. The high removal efficiency of RB19 in synthetic dye bath solution by LC- Al_2O_3 biosorbent indicates the great application potential of the biosorbent in removing anionic dye from water.

Comparative analysis of sorption capacity of various sorbents for simultaneous removal

For the purpose of comparison of the LC- Al_2O_3 biosorption capacity for simultaneous removal of different types of pollutants, Table 4 presents the maximum sorption capacity of the LC- Al_2O_3 biosorbent for simultaneous removal of Cu(II) ions, RB19 and cyprodinil with data for the maximum sorption capacity for other pollutants simultaneously removed in a multi-component system by different sorbents reported in the literature. The sorption capacity depends on the nature of sorbent material and modification, conditions and type of pollutant.

It is clear from Table 4 that sorption capacities for the simultaneous sorption of pollutants depend on sorbent nature and condition in which the pollutants can be removed simultaneously in a multi-component system. The organoclay sorbents are the dominant type of sorbents for simultaneous removal of the pollutants with high sorbent capacity. On the other hand, it is noticeable that LC- Al_2O_3 biosorbent shows interesting sorption potential among the rest of the sorbents for simultaneous removal of pollutants and also possesses other benefits like cost-effectiveness of wood residue, easy sorbent preparation, biocompatibility and environmental-friendliness.

Economical aspects

The use of sorbents is one of the alternative options, when traditional wastewater treatment methods, such as biological treatment or chemical precipitation, cannot be used because of the high costs, low removal efficiency and a large amount of chemicals used or sludge produced. Although popular options for sorbents, such as activated carbon, provide high sorption capacities for a wide range of sorbates, developing possibilities for cheaper alternatives is still in need. Biosorbents based on biomass and obtained by its modifications have been used predominantly for efficient removal of metal cations from water. In an attempt to improve biosorbents based on lignocellulose to remove not only metal cations but also organic pollutants from water, a new biosorbent was synthesized based on the chemical modification with a small amount of Al_2O_3 . The new biosorbent kept the ability to remove cations and succeeded to remove nonpolar and anionic organic pollutants. In this way, the biosorbent got the characteristics which have more expensive activated carbons. Activated carbon, which is present on the market in powdered and granular form, has a value between 600 and 2000 USD/t on average. Wood residue, as a precursor for the production of chemically modified lignocellulosic biosorbent with Al_2O_3 , is considered as an extremely economical resource. Woodchips were generated from furniture manufacturing, so in that manner, besides being free, waste can be reduced and reuse options of woodchips increased. Further chemical modification

Table 4 Comparison of sorption capacity of various sorbents used to simultaneously remove pollutants in multi-component system

Sorbent	Pollutants	Q_m (mg g ⁻¹)	pH	Source
Modified masau stones	Cr(VI)	66.99	3.5	Albadarin et al. (2017)
	Orange II	129.2		
Modified tannery waste	Cr(VI)	59.43	3.5	Anandkumar and Mandal (2011)
	Rhodamine B	106.29		
Grafted chitosan	Cr(VI)	22.1	4.0	Kyzas et al. (2013)
	Remazol red 3	447.53		
Modified chitosan	Cr(VI)	3.29	3.29	Li et al. (2016)
	Methyl orange	2.54		
Bentonite clay	Zn(II)	5.68	5.0	Oyanedel-Craver et al. (2007)
	Benzene	5.87		
Metal–organic composite	Pb(II)	219.00	–	Shi et al. (2018)
	Malachite green	113.67		
Metal–organic composite	Pb(II)	102.0	4.0	Huang et al. (2018)
	Methylene blue	128.0		
Bentonite clay	Pb(II)	41.36	5.0	Oyanedel-Craver et al. (2007)
	Benzene	6.44		
Organoclays	Pb(II)	33.78	–	Huang et al. (2015)
	2,4-D	96.15		
Carbon nanotubes	Cu(II)	38.91	6.0	Tang et al. (2012)
	Atrazine	40.16		
Bentonite	Cu(II)	23.07	6.5	Jin et al. (2016)
	2,4-D	16.22		
Organoclays	Cu(II)	19.01	6.0	Jin et al. (2014)
	Amoxicillin	24.39		
Organo-montmorillonite	Cu(II)	14.12	5.0	Ma et al. (2016a, b)
	Phenol	9.90		
Organo-montmorillonite	Cu(II)	3.75	5.0	Ma et al. (2016a, b)
	Phenol	13.76		
Modified palygorskite	Cu(II)	1.00	–	Wang et al. (2015)
	Methylene blue	173.3		
Aerobic activate sludge	Ni(II)	168.0	1.0	Aksu and Akpınar (2000)
	Phenol	166.6		
Aerobic activate sludge	Ni(II)	145.8	4.5	Aksu and Akpınar (2000)
	Phenol	208.3		
Modified bentonite	Cd(II)	36.96	–	Sun et al. (2014)
	Phenol	36.77		
Bentonite clay	Cd(II)	7.44	5.0	Oyanedel-Craver et al. (2007)
	Benzene	7.10		
Silica	Reactive black 5	83.33	2.0	Araghi and Entezari (2015)
	Na dodecylbenzenesulfonate	62.5		

Table 4 (continued)

Sorbent	Pollutants	Q_m (mg g ⁻¹)	pH	Source
Bentonite	Methyl orange	5.37	4.5	Leodopoulos et al. (2012)
	Humic acid	2.1		
Graphene oxide nanocomposite	Cd(II)	21.38	6.0	Deng et al. (2013)
	Methylene blue	64.23		
Graphene oxide nanocomposite	Cd(II)	91.29	6.0	Deng et al. (2013)
	Orange G	20.85		
Organo-montmorillonite	Cd(II)	15.27	5.0	Ma et al. (2016a, b)
	Phenol	8.34		
	Phosphate	13.04		
Lignocellulosic-Al ₂ O ₃	Cu(II)	15.69	5.0	This study
	Reactive Blue 19	29.99		
	Cyprodinil	20.97		

of woodchips to a final biosorbent product comprises only the costs of a few cheap chemicals and electric energy used for stirring. So, the final cost of the obtained biosorbent is estimated to less than 300 USD/t, making it very interesting in the light of its commercialization and practical usage in the future.

Conclusion

A new biosorbent, hybrid material, based on chemical modification of lignocellulosic biomass with Al₂O₃ was synthesized. As a starting biomass, woodchips from an oak tree (*Quercus robur*) generated from furniture manufacturing were used. In that manner, wood waste could be reduced, and reuse/recycle options of woodchips were increased. Chemical modification of the biosorbent was confirmed by FTIR spectrum analysis. SEM micrographs showed that the chemical modification did not change the morphological structure of the biomaterial. The EDX analysis showed the presence of 32.8% of carbon and 52.5% of oxygen with 14.7% aluminum. No separate crystalline Al₂O₃ phase was detected in LC-Al₂O₃ by the XRD pattern, further indicating and confirming the chemical interaction between Al₂O₃ and the biomaterial functional groups. LC-Al₂O₃ biosorbent was successfully used for simultaneous removal of cationic (Cu(II) ion), anionic (textile dye RB19) and nonpolar (pesticide cyprodinil) pollutants from model solutions and natural water. The optimal pH value, where all three types of pollutant can be simultaneously removed with enough high efficiency, is 5. At this pH value, removal efficiency for Cu(II) ions, RB19 and cyprodinil is 98.21%, 97.9% and 98.18%, respectively. It can be assumed that the main binding mechanism is ion exchange in the case of Cu(II) and RB19, and in the case of nonpolar cyprodinil molecule, the mechanism of sorption process has a physicochemical nature. The effect of temperature shows that the biosorption process for Cu(II) and RB19 was endothermic and for cyprodinil exothermic in nature. The optimal biosorbent dose for LC-Al₂O₃ was 2.0 g dm⁻³. The sorption

process followed the pseudo-second-order model, intraparticle and Chrastil's diffusion model in all three cases, indicating that both kinetics, reaction and diffusion, can be involved in the biosorption process. The Langmuir isotherm model showed the best fit to experimental data in describing the sorption of all three pollutants on biosorbent. The simultaneous removal of all three pollutants from the aqueous model solution and contaminated river water at optimal parameters was very efficient, and the *RE* % was the same as that achieved in single model solutions (98.21, 97.9 and 98.18% for Cu(II) ions, RB19 and cyprodinil, respectively), indicating that there was no mutual influence of pollutants on each other. The maximal sorption capacities of the LC-Al₂O₃ biosorbent for simultaneous removal of the pollutants in the multi-component system are 15.69 mg g⁻¹ for Cu(II) ions, 29.99 mg g⁻¹ for RB19 and 20.97 mg g⁻¹ for cyprodinil. In addition to the high removal efficiency for different types of pollutants (cationic, anionic and nonpolar), LC-Al₂O₃ biosorbent possesses other benefits, like cost-effectiveness of wood residue and low-cost and easy sorbent preparation, making it a promising material for the removal of different types of pollutants from water and wastewaters.

Acknowledgements This work was financed by the Serbian Ministry of Education, Science and Technological Development through the Grant No TR34008.

Compliance with ethical standards

Conflict of interest The authors declare that they have no conflict of interest.

References

- Abdolali A, Ngo HH, Guo W, Zhou JL, Du B, Wei Q, Wang XC, Nguyen PD (2015) Characterization of a multi-metal binding biosorbent: chemical modification and desorption studies. *Bioresour Technol* 193:477–487
- Akbari M, Hallajisani A, Keshtkar AR, Shahbeig H, Ghorbanian SA (2015) Equilibrium and kinetic study and modeling of Cu(II) and Co(II) synergistic biosorption from Cu(II)-Co(II) single and binary mixtures on brown algae *C. indica*. *J Environ Chem Eng* 3:140–149
- Aksu Z, Akpinar D (2000) Modelling of simultaneous biosorption of phenol and nickel(II) onto dried aerobic activated sludge. *Sep Purif Technol* 21(1–2):87–99
- Albadarin AB, Solomon S, Kurniawan TA, Mangwandi C, Walker G (2017) Single, simultaneous and consecutive biosorption of Cr(VI) and Orange II onto chemically modified masau stones. *J Environ Manag* 204:365–374
- Albert Q, Leleyter L, Lemoine M, Heutte N, Rioult J-P, Sage L, Baraud F, Garon D (2018) Comparison of tolerance and biosorption of three trace metals (Cd, Cu, Pb) by the soil fungus *Absidia cylindrospora*. *Chemosphere* 196:386–392
- Alqadami AA, Naushad M, Alothman ZA, Ghfar AA (2017) Novel metal-organic framework (MOF) based composite material for the sequestration of U(VI) and Th(IV) metal ions from aqueous environment. *ACS Appl Mater Interfaces* 9:36026–36037
- Alqadami AA, Naushad M, Alothman ZA, Ahamad T (2018) Adsorptive performance of MOF nanocomposite for methylene blue and malachite green dyes: kinetics, isotherm and mechanism. *J Environ Manage* 223:29–36
- Amirnia S, Ray MB, Margaritis A (2016) Copper ion removal by *Acer saccharum* leaves in a regenerable continuous-flow column. *Chem Eng J* 287:755–764
- Anandkumar J, Mandal B (2011) Adsorption of chromium(VI) and Rhodamine B by surface modified tannery waste: kinetic, mechanistic and thermodynamic studies. *J Hazard Mater* 186:1088–1096

- Araghi SH, Entezari MH (2015) Amino-functionalized silica magnetite nanoparticles for the simultaneous removal of pollutants from aqueous solution. *Appl Surf Sci* 333:68–77
- Ayoob S, Gupta AK, Bhakat PB, Bhat VT (2007) Investigations on the kinetics and mechanisms of sorptive removal of fluoride from water using alumina cement granules. *Chem Eng J* 140:6–14
- Bektaş N, Aydın S, Öncel MS (2011) The adsorption of arsenic ions using beidellite, zeolite, and sepiolite clays: a study of kinetic, equilibrium and thermodynamics. *Sep Sci Technol* 46:1005–1016
- Berrazoum A, Marouf R, Oudjenia F, Schott J (2015) Bioadsorption of a reactive dye from aqueous solution by municipal solid waste. *Biotechnol Rep* 7:44–50
- Bozbas SK, Boz Y (2016) Low-cost biosorbent: *anadara inaequalis* shells for removal of Pb(II) and Cu(II) from aqueous solution. *Process Saf Environ Prot* 103:144–152
- Chaudhuri H, Dash S, Ghorai S, Pal S, Sarkar A (2016) SBA-16: application for the removal of neutral, cationic, and anionic dyes from aqueous medium. *J Environ Chem Eng* 4:157–166
- Chrastil J (1990) Adsorption of direct dyes on cotton: kinetics of dyeing from finite baths based on new information. *Text Res J* 60:413–416
- Daneshvar E, Vazirzadeh A, Niazi A, Kousha M, Naushad M, Bhatnagar A (2017) Desorption of methylene blue dye from brown macroalgae: effects of operating parameters, isotherm study and kinetic modeling. *J Clean Prod* 152:443–453
- Deng JH, Zhang XR, Zeng GM, Gong JL, Niu QY, Liang J (2013) Simultaneous removal of Cd (II) and ionic dyes from aqueous solution using magnetic graphene oxide nanocomposite as an adsorbent. *Chem Eng J* 226:189–200
- El-Sakhawy M (2001) Characterization of modified oxycellulose. *J Therm Anal Cal* 63:549–558
- Entezari MH, Soltani T (2008) Simultaneous removal of copper and lead ions from a binary solution by sono-sorption process. *J Hazard Mater* 160:88–93
- Freundlich HZ (1906) Over the adsorption in solution. *J Phys Chem* 57A:385–470
- Ho YS, McKay G (1998) Kinetic models for the sorption of dye from aqueous solution by wood. *Process Saf Environ Prot* 76:183–191
- Ho YS, McKay G (2000) The kinetics of sorption of divalent metal ions onto sphagnum moss peat. *Water Res* 34:735–742
- Huang L, Zhou Y, Guo X, Chen Z (2015) Simultaneous removal of 2,4-dichlorophenol and Pb(II) from aqueous solution using organoclays: isotherm, kinetics and mechanism. *J Ind Eng Chem* 22:280–287
- Huang L, He M, Chen B, Hu B (2018) Magnetic Zr-MOFs nanocomposites for rapid removal of heavy metal ions and dyes from water. *Chemosphere* 199:435–444
- Isah AU, Abdurraheem G, Bala S, Muhammad S, Abdullahi M (2015) Kinetics, equilibrium and thermodynamics studies of C.I. Reactive Blue 19 dye adsorption on coconut shell based activated carbon. *Int Biodeterior Biodegrad* 102:265–273
- Javadian H, Angaji MT, Naushad M (2014) Synthesis and characterization of polyaniline/ γ -alumina nanocomposite: a comparative study for the adsorption of three different anionic dyes. *J Ind Eng Chem* 20:3890–3900
- Jin X, Zha S, Li S, Chen Z (2014) Simultaneous removal of mixed contaminants by organoclays—amoxicillin and Cu(II) from aqueous solution. *Appl Clay Sci* 102:196–201
- Jin X, Zheng M, Sarkar B, Naidu R, Chen Z (2016) Characterization of bentonite modified with humic acid for the removal of Cu (II) and 2,4-dichlorophenol from aqueous solution. *Appl Clay Sci* 134:89–94
- Kallel F, Bouaziz F, Chaari F, Belghith L, Ghorbel R, Chaabouni SE (2016) Interactive effect of garlic straw on the sorption and desorption of Direct Red 80 from aqueous solution. *Process Saf Environ Prot* 102:30–43
- Kumar PM, Balasubramanian C, Sali ND, Bhoraskar SV, Rohatgi VK, Badrinarayanan S (1999) Nanophase alumina synthesis in thermal arc plasma and characterization: correlation to gas-phase studies. *Mater Sci Eng, B* 63:215–227
- Kyzas GZ, Lazaridis NK, Kostoglou M (2013) On the simultaneous adsorption of a reactive dye and hexavalent chromium from aqueous solutions onto grafted chitosan. *J Colloid Interface Sci* 407:432–441
- Lagergren S (1898) Zur Theorie der sogenannten Adsorption gelöster Stoffe (About the theory of so-called adsorption of soluble substances). *Kungliga Svenska Vetenskapsakademiens Handl* 24:1–39
- Langmuir I (1918) The adsorption of gases on plane surfaces of glass, mica and platinum. *J Am Chem Soc* 40:1361–1403

- Lazar T (2005) Color chemistry: synthesis, properties, and applications of organic dyes and pigments. Wiley Online Library, New York
- Leodopoulos C, Doulia D, Gimouhopoulos K, Triantis TM (2012) Single and simultaneous adsorption of methyl orange and humic acid onto bentonite. *App Clay Sci* 70:84–90
- Li K, Li P, Cai J, Xiao S, Yang H, Li A (2016) Efficient adsorption of both methyl orange and chromium from their aqueous mixtures using a quaternary ammonium salt modified chitosan magnetic composite adsorbent. *Chemosphere* 154:310–318
- Liu Y (2006) Some consideration on the Langmuir isotherm equation. *Colloid Surface A* 274:34–36
- Liu Y (2009) Is the free energy change of adsorption correctly calculated? *J Chem Eng Data* 54:1981–1985
- Liu Y, Liu K, Zhang L, Zhang Z (2015) Removal of Rhodamine B from aqueous solution using magnetic NiFe nanoparticles. *Water Sci Technol* 72:1243–1249
- Ma L, Chen Q, Zhu J, Xi Y, He H, Zhu R, Tao Q, Ayoko GA (2016a) Adsorption of phenol and Cu(II) onto cationic and zwitterionic surfactant modified montmorillonite in single and binary systems. *Chem Eng J* 283:880–888
- Ma L, Zhu J, Xi Y, Zhu R, He H, Liang X, Ayoko GA (2016b) Adsorption of phenol, phosphate and Cd(II) by inorganic–organic montmorillonites: a comparative study of single and multiple solute. *Colloids Surf A* 497:63–71
- Naushad M, Abdullah ALOthman Z, Rabiul Awual M, Alfadul SM, Ahamad T (2015) Adsorption of rose Bengal dye from aqueous solution by amberlite Ira-938 resin: kinetics, isotherms, and thermodynamic studies. *Desalin Water Treat* 57:13527–13533
- Naushad M, Ahamad T, Al-Maswari BM, Alqadami AA, Alshehri SM (2017) Nickel ferrite bearing nitrogen-doped mesoporous carbon as efficient adsorbent for the removal of highly toxic metal ion from aqueous medium. *Chem Eng J* 330:1351–1360
- Oyanedel-Craver VA, Fuller M, Smith JA (2007) Simultaneous sorption of benzene and heavy metals onto two organoclays. *J Colloid Interface Sci* 309(2):485–492
- Pettersen RC (1984) The chemistry of solid wood. *Advances in chemistry*. Chapter 2: the chemical composition of wood. American Chemical Society, Washington, DC
- Pionke HB, Glotfelty DW (1990) Contamination of groundwater by atrazine and selected metabolites. *Chemosphere* 21:813–822
- Roonasi P, Nezhad AY (2016) A comparative study of a series of ferrite nanoparticles as heterogeneous catalysts for phenol removal at neutral pH. *Mater Chem Phys* 172:143–149
- Santos SCR, Boaventura RAR (2016) Adsorption of cationic and anionic azo dyes on sepiolite clay: equilibrium and kinetic studies in batch mode. *J Environ Chem Eng* 4:1473–1483
- Shakib F, Koochi AD, Pirzaman AK (2017) Adsorption of methylene blue by using novel chitosan-g-itaconic acid/bentonite nanocomposite: equilibrium and kinetic study. *Water Sci Technol* 75:1932–1943
- Shi Z, Xu C, Guan H, Li L, Fan L, Wang Y, Liu L, Meng Q, Zhang R (2018) Magnetic metal organic frameworks (MOFs) composite for removal of lead and malachite green in wastewater. *Colloids Surf. A Physicochem. Eng. Asp.* 539:382–390
- Sips R (1948) On the structure of a catalyst surface. *J Chem Phys* 16:490–495
- Sun Y-X, Li X-R, Zhao Y-Y, Li C-Y, Ren Z-L (2014) Simultaneous sorption of Cd²⁺ and phenol to CTMAB-CA modified bentonite from aqueous solutions. *Adv Appl Sci Res* 5:155–158
- Tang WW, Zeng GM, Gong JL, Liu Y, Wang XY, Liu YY, Liu ZF, Chen L, Zhang XR, Tu DZ (2012) Simultaneous adsorption of atrazine and Cu (II) from wastewater by magnetic multi-walled carbon nanotube. *Chem Eng J* 211:470–478
- Todorciuc T, Bulgariu L, Popa IV (2015) Adsorption of Cu(II) from aqueous solution on wheat straw lignin: equilibrium and kinetic studies. *Cell Chem Technol* 49:439–447
- Tural B, Ertaş E, Enez B, Fincan SA, Tural S (2017) Preparation and characterization of a novel magnetic biosorbent functionalized with biomass of *Bacillus Subtilis*: kinetic and isotherm studies of biosorption processes in the removal of Methylene Blue. *J Environ Chem Eng* 5:4795–4802
- Vaquero-Fernández L, Sáenz-Hernández A, Sanz-Asensio J, Fernández-Zurbano P, Sainz-Ramírez M, Pons-Jubera B, López-Alonso M, Epifanio-Fernández S-I, Martínez-Soria M-T (2008) Determination of cyprodinil and fludioxonil in the fermentative process of must by high-performance liquid chromatography-diode array detection. *J Sci Food Agric* 88:1943–1948
- Vázquez-Guerrero A, Alfaro-Cuevas-Villanueva R, Rutiaga-Quiñones JG, Cortés-Martínez R (2016) Fluoride removal by aluminum-modified pine sawdust: effect of competitive ions. *Ecol Eng* 94:365–379

- Wang W, Tian G, Zhang Z, Wang A (2015) A simple hydrothermal approach to modify palygorskite for high-efficient adsorption of methylene blue and Cu(II) ions. *Chem Eng J* 265:228–238
- Weber WJ Jr, Morris JC (1964) Kinetics of adsorption on carbon from solution. *J Sanit Eng Div* 89:31–60
- Wibowo E, Rokhmat M, Sutisna Khairurrijal K, Abdullah M (2017) Reduction of seawater salinity by natural zeolite (Clinoptilolite): adsorption isotherms, thermodynamics and kinetics. *Desalination* 409:146–156

Publisher's Note Springer Nature remains neutral with regard to jurisdictional claims in published maps and institutional affiliations.